NASA/TM—2010-216751

Experimental Charging Behavior of Orion UltraFlex Array Designs

Joel T. Galofaro
Glenn Research Center, Cleveland, Ohio

Boris V. Vayner
Ohio Aerospace Institute, Brook Park, Ohio

Grover B. Hillard
Glenn Research Center, Cleveland, Ohio

May 2010

NASA STI Program . . . in Profile

Since its founding, NASA has been dedicated to the advancement of aeronautics and space science. The NASA Scientific and Technical Information (STI) program plays a key part in helping NASA maintain this important role.

The NASA STI Program operates under the auspices of the Agency Chief Information Officer. It collects, organizes, provides for archiving, and disseminates NASA's STI. The NASA STI program provides access to the NASA Aeronautics and Space Database and its public interface, the NASA Technical Reports Server, thus providing one of the largest collections of aeronautical and space science STI in the world. Results are published in both non-NASA channels and by NASA in the NASA STI Report Series, which includes the following report types:

- TECHNICAL PUBLICATION. Reports of completed research or a major significant phase of research that present the results of NASA programs and include extensive data or theoretical analysis. Includes compilations of significant scientific and technical data and information deemed to be of continuing reference value. NASA counterpart of peer-reviewed formal professional papers but has less stringent limitations on manuscript length and extent of graphic presentations.

- TECHNICAL MEMORANDUM. Scientific and technical findings that are preliminary or of specialized interest, e.g., quick release reports, working papers, and bibliographies that contain minimal annotation. Does not contain extensive analysis.

- CONTRACTOR REPORT. Scientific and technical findings by NASA-sponsored contractors and grantees.

- CONFERENCE PUBLICATION. Collected papers from scientific and technical conferences, symposia, seminars, or other meetings sponsored or cosponsored by NASA.

- SPECIAL PUBLICATION. Scientific, technical, or historical information from NASA programs, projects, and missions, often concerned with subjects having substantial public interest.

- TECHNICAL TRANSLATION. English-language translations of foreign scientific and technical material pertinent to NASA's mission.

Specialized services also include creating custom thesauri, building customized databases, organizing and publishing research results.

For more information about the NASA STI program, see the following:

- Access the NASA STI program home page at *http://www.sti.nasa.gov*

- E-mail your question via the Internet to *help@sti.nasa.gov*

- Fax your question to the NASA STI Help Desk at 443–757–5803

- Telephone the NASA STI Help Desk at 443–757–5802

- Write to:
  NASA Center for AeroSpace Information (CASI)
  7115 Standard Drive
  Hanover, MD 21076–1320

NASA/TM—2010-216751

Experimental Charging Behavior of Orion UltraFlex Array Designs

Joel T. Galofaro
Glenn Research Center, Cleveland, Ohio

Boris V. Vayner
Ohio Aerospace Institute, Brook Park, Ohio

Grover B. Hillard
Glenn Research Center, Cleveland, Ohio

National Aeronautics and
Space Administration

Glenn Research Center
Cleveland, Ohio 44135

May 2010

Acknowledgments

The authors wish to express their gratitude to the following companies for supplying the needed CIC assemblies and technical specifications for these experiments: Lockheed-Martin Corporation (prime contractor for integration of UltraFlex Arrays on CEV), ATK Space Systems in Goleta California (subcontractor for design/fabrication of Orion UltraFlex Arrays on CEV), Emcore Corporation (ZTJM CIC manufacturer), and Spectrolab a subsidiary of Boeing (XTJ CIC manufacturer).

Level of Review: This material has been technically reviewed by technical management.

Available from

NASA Center for Aerospace Information
7115 Standard Drive
Hanover, MD 21076–1320

National Technical Information Service
5301 Shawnee Road
Alexandria, VA 22312

Available electronically at http://gltrs.grc.nasa.gov

Experimental Charging Behavior of Orion UltraFlex Array Designs

Joel T. Galofaro
National Aeronautics and Space Administration
Glenn Research Center
Cleveland, Ohio 44135

Boris V. Vayner
Ohio Aerospace Institute
Brook Park, Ohio 44142

Grover B. Hillard
National Aeronautics and Space Administration
Glenn Research Center
Cleveland, Ohio 44135

Abstract

The present ground based investigations give the first definitive look describing the charging behavior of Orion UltraFlex arrays in both the Low Earth Orbital (LEO) and geosynchronous (GEO) environments. Note the LEO charging environment also applies to the International Space Station (ISS). The GEO charging environment includes the bounding case for all lunar mission environments. The UltraFlex photovoltaic array technology is targeted to become the sole power system for life support and on-orbit power for the manned Orion Crew Exploration Vehicle (CEV). The purpose of the experimental tests is to gain an understanding of the complex charging behavior to answer some of the basic performance and survivability issues to ascertain if a single UltraFlex array design will be able to cope with the projected worst case LEO and GEO charging environments. Stage 1 LEO plasma testing revealed that all four arrays successfully passed arc threshold bias tests down to –240 V. Stage 2 GEO electron gun charging tests revealed that only front side area of indium tin oxide coated array designs successfully passed the arc frequency tests.

Nomenclature

E_B	beam energy, (keV)
I_c	collected string current, (A)
I_D	Beam current density, (nA/cm^2)
I_p	String parasitic current loss percentage
I_{pv}	string peak current, (A)
N_e	electron number density, (cm^{-3})
T_e	electron temperature, (eV)
V_B	array bias potential, (kV)
V_f	floating potential, (V)
V_{op}	array string operating voltage, (V)
V_p	plasma potential, (V)
V_{pv}	string peak voltage, (V)

Introduction

The Orion old 28 V and present 120 V UltraFlex arrays, designed by ATK Space Systems of Goleta, California under subcontract to Orion prime contractor, Lockheed-Martin Corporation, represent a unique design challenge (Refs. 1 to 5). The array designs will encounter a number of different space environments ranging from LEO to cis-lunar with brief passage through the Van Allen Belts, and the lunar orbital environments. Fortunately, all cis-lunar and lunar mission environments can be effectively categorized under a broader category termed the geosynchronous environment case. Thus, there are only two spacecraft environments that apply: LEO and GEO.

Traditionally, photovoltaic arrays are designed for a single environment. For the Orion mission, a single array design is needed for operation in both LEO and GEO space environments. Preliminary risk identification for the Crew Exploration Vehicle (CEV) was made early on by the Orion Project Team (Ref. 6). The Orion Team study pointed to four major issues (1) Atomic oxygen degradation of ITO coatings in LEO, (2) ESD breakdown of dielectric coatings in GEO during geomagnetic substorm events, (3) Electrostatic Discharge (ESD) due to pinholes or damage caused by micro-meteorite impacts or orbital debris, and (4) sputtering of ITO coatings and related array contamination.

LEO deployment and operations involve exposure to relatively cold dense plasma with well-known interactions issues: floating potential shifts, parasitic power loss, arcing, and atomic oxygen sputtering. Parasitic current collection and the resulting associated power losses from the array is closely related to a highly nonlinear phenomenon termed snapover (Refs. 6 to 8). Under snapover conditions a small pinhole in dielectric can collect current as much as would be the case if the entire surface were conductive. Thus, high voltage Orion array must be tested against sudden increase in current collection. The ISS floating potential probe measurements revealed potential spikes of 40 V negative can present danger of arcing to an astronaut's space suit (Refs. 9 to 11). The addition of new solar arrays to ISS and deployment of high voltage Orion solar arrays in LEO demand reevaluation of floating potential peaks and differential charging on CEV surfaces.

The GEO environment is characterized as relatively low-density plasma with high energy particles (protons and electrons) subject to violent magnetic storms (Refs. 6 and 12). As a spacecraft passes through the substorm environment, differential charging can reach a few kilovolts, which create danger of powerful electrostatic discharge. During its course to cis-lunar orbital space the Orion spacecraft will basically see three GEO space charging environments; spending approximately 73.5 percent of its time in the Solar Wind, 13.3 percent of its time in the Earth's Magnetosheath, and about 13.2 percent of its time in the Earth's Magnetotail. Table 1 gives a comparison of worst case charging environments (Refs. 6 and 12).

TABLE 1.—WORST CASE GEO CHARGING ENVIRONMENTS

	Design case	Solar wind	Magneto-sheath	Magneto-tail
Electron density, cm^{-3}	1.12	9.5	1.1	0.16
Electron temperature, eV	1.2×10^4	12.1	26.9	145.6
Proton density, cm^{-3}	0.24	8.7	1	0.15
Proton temperature, eV	2.95×10^4	10.3	79.9	610.1

The general practice for spacecraft designers has been to use a single spacecraft design for operation in LEO and separate spacecraft design for operation in the GEO environment. As a result, the common practice of photovoltaic array manufacturers is to force the array cell SiO_2 cover slide to become conducting by over-coating the insulating cover with a thin layer of Indium Tin Oxide (ITO) for operation in the GEO environment. Because a single Orion array design is required for operation in both LEO and GEO environments, the consensus made by the Orion CEV Project Team was to apply ITO coatings on each of the photovoltaic array surfaces. The Orion arrays are also required to have Anti-Reflective (AR) Magnesium Fluoride (MgF_2) coatings over ITO layers on each cell. These MgF_2 layers have a thickness of ~0.1 μm defined by the optical requirements. Results from ground tests clearly demonstrated that the AR resistivity (~10^9 Ω per square) is low enough to bleed off charge in the GEO environment.

The reported tests of the new UltraFlex arrays designs are the first of their kind detailing the expected charging behavior under extreme LEO and GEO environments. First and foremost, the purpose of the current experimental research is to ascertain if each of the manufactured array cell types can satisfactorily perform Electrostatic Discharge (ESD) free under worst case LEO and GEO charging conditions. Secondly, the reported research will be used to determine if a single array design can be effectively used for operation in both the LEO and GEO flight regimes, to determine the relative strength and weakness of each of the different manufactured array cells, with the expressed intent of deciding in the very near future which array cell manufacturer will be chosen for integration in the final Orion CEV UltraFlex array design.

Experimental Apparatus

Tests were conducted in the Plasma Interaction Facility's Tenney Charging Simulator (VF-20) chamber (see Fig. 1 for details). (Vacuum chamber dimensions: 1.8 m diameter by 1.5 m length). The chamber is equipped with large 0.9 m diameter cryogenic pump that provides a background pressure of 2×10^{-7} torr. A digital ionization gauge was used to monitor the chamber pressure. The chamber is equipped with a Kaufman type discharge source that ionizes xenon gas neutrals via a hot filament cathode. The xenon discharge source was used to simulate the electrical charging conditions encountered in the LEO environment. Tank pressure was adjusted by slowly bleeding xenon gas neutrals into the chamber until a pressure of 5.0×10^{-5} torr was achieved with the discharge source operating. Plasma parameters were obtained by sweeping a Langmuir Probe ($N_e = 3.510^6$ cm^{-3}, $T_e = 0.25$ eV). For GEO testing the vacuum chamber was pumped down to the base tank pressure and the array assemblies were allowed to outgas in the chamber for a minimum of 8 hr prior to testing. Two electron guns with matching 0 to 20 kV power supplies are mounted at the far end of the chamber and pointed at the array. GEO charging was simulated by irradiating the CIC assemblies with e-beams (~1 nA/cm^2 current density). A two-dimensional (2–D) positioning system was installed in front of the array. The 2–D positioning system carried an electrostatic noncontact probe for measuring potentials on the surfaces of the array and also included a Faraday Cup for measuring beam current density. A digital high impedance voltmeter was used to plot and save probe potential distribution via a laptop computer. In principal, only the source-facing side of the array can be tested at a time because of wake effects caused by shadowing of the backward facing array surfaces. Therefore, the vacuum chamber needs to be reopened and the array flipped for retesting the back side array surfaces.

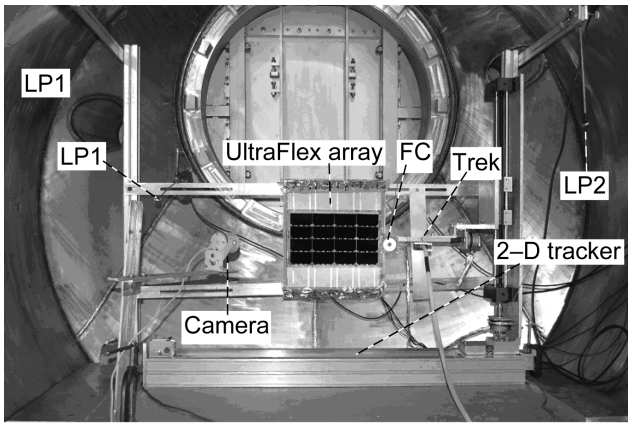

Figure 1.—Snapshot showing Tenney Charging Simulator VF-20 Chamber.

Array testing was limited to just four individual development level assemblies, two each from two different cell manufacturers. One array manufacturer provided assemblies with series Z Triple Junction Monolithic (ZTJM) cell design one Anti Reflection (AR) coated "AR-ZTJM" and one with an Indium Tin Oxide (ITO) coatings "AR-ITO-ZTJM". The second array manufacturer provided assemblies contained the next generation series X Triple Junction (XTJ) assemblies: one with an AR coating "AR-XTJ" and one with an ITO coating "AR-ITO-XTJ". Although not included on the CICs assemblies that were tested the flight solar array strings incorporate blocking diodes that act to limit current in the case of sustained arcing between adjacent strings. (The array assemblies tested have thinned germanium substrates: thinned from 140 to 100 μm thick ZTJM and 110 μm thick XTJ which was designed to save wing mass.)

The layout of each of the four assemblies was identical: four parallel strings with four Cells in Circuit (CIC) assemblies per string wired in series. An insulating, silicone encapsulated Vectran gore mesh was attached to a rigid insulating composite fiberglass (G-11) frame with the CICs cemented directly to the Vectran mesh. (Mesh encapsulates are CV2568 for the ZTJM array and CV2566 for the XTJ array.) ZTJM arrays used thin conductive strips for each string output lead. The thin conductive strips are brought out to the edge of the frame and terminated via string termination pads. All conducting strips have a thin insulating layer of Tedlar covering each conductive strip. See Figures 2(a) to (d) for details. The XTJ arrays had no conductive strips. XTJ arrays also had a thin insulating Kapton sheet masking off the non cell areas. The back side of CICs were primed with silicone adhesive by dabbing small amounts of silicone to promote adhesion but leaving some areas of the conductor exposed. Also areas between the strings are not grouted on all four array CIC assemblies tested.

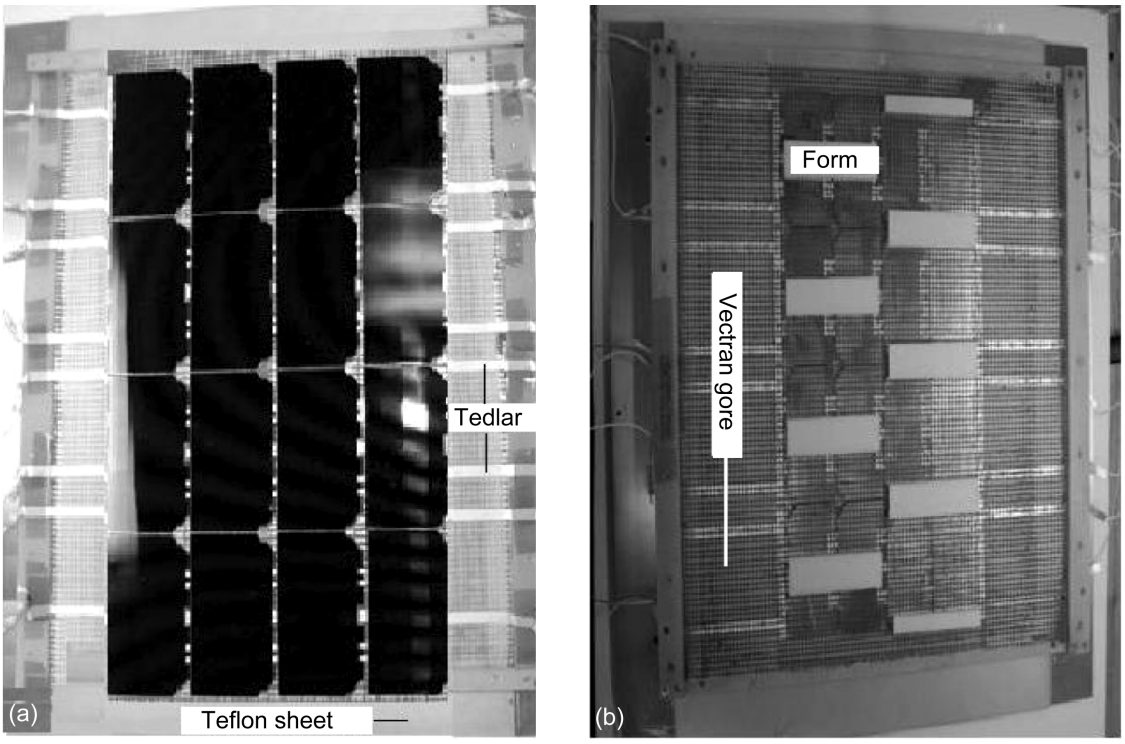

Figure 2.—(a) Front side of UltraFlex array with AR-ZTJM CICs. (b) Back side of UltraFlex array, with AR-ZTJM CICs.

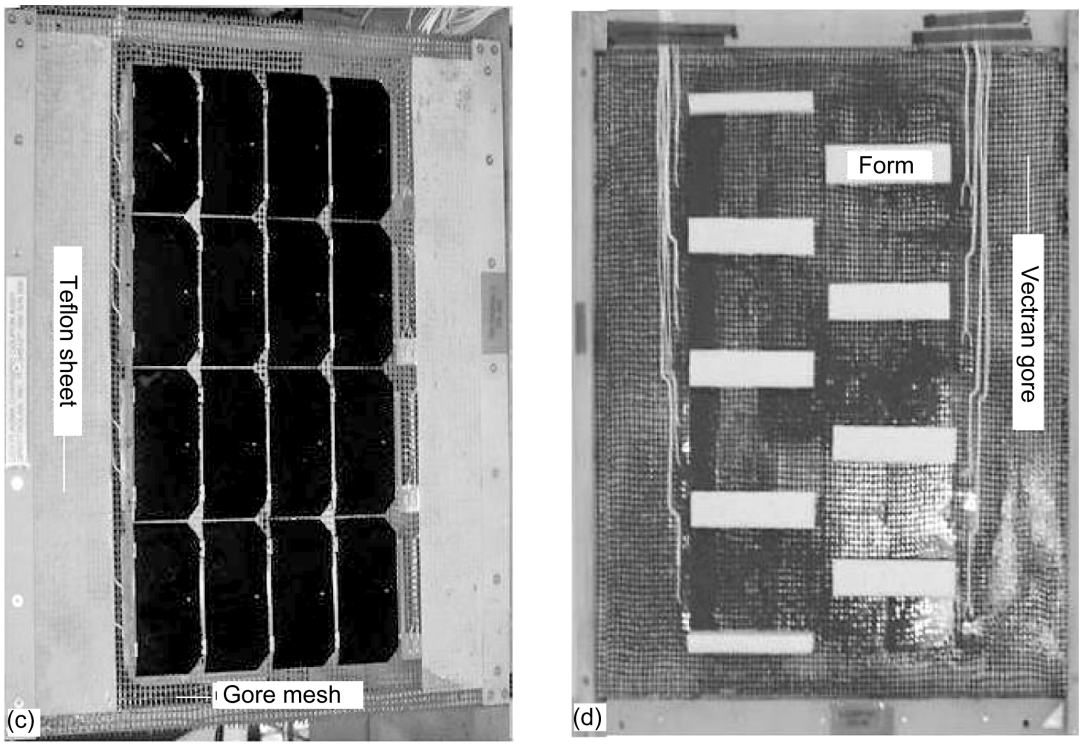

Figure 2.—Concluded. (c) Front side of UltraFlex array with AR-XTJ CICs. (d) Back side of UltraFlex array with AR-XTJ CICs.

Circuitry diagrams for testing against ESD inception in both LEO and GEO environments is shown below. Figure 3(a) shows an R-C circuit, current probe and current probe amplifier which is used to detect primary arcs on the array. An oscilloscope control program code arms the scope and sets the trigger state to ready. When an arc occurred and exceeded a pre-programmed trigger level, waveform data is recorded to a specified file on the computer and the scope is then switched back to an auto ready mode awaiting the next arc event. If an arc occurs between two adjacent array strings the setup in Figure 3(b) would be used to check for sustained arcs. A Solar Array Simulator (SAS) power supply with predetermined voltage and current limits is placed between two adjacent array strings where the primary arc was first detected. A color video camera is mounted inside the vacuum chamber and a video recorder is used to recording arcs. Additionally a quadrupole mass spectrometer was used to monitor gas species in the chamber.

LEO and GEO Test Procedures

The following test plan sequence started on delivery of each solar array sample: Photographs of the front and back side of the array were taken prior to testing followed by visual inspections to document any anomalies during shipment. Arrays were then delivered to our Cell Calibration Flash Simulator Laboratory to make a baseline performance measurement at room temperature prior to ESD testing. Measurements of short circuit current, open circuit voltage, maximum voltage, maximum current, maximum power and cell efficiency were performed on each array string. The array was then delivered to the Atomic Oxygen Facility for a front side exposure of the anti-reflection (AR) (or AR/ITO) coatings to measure the performance degradation under Atomic Oxygen (AO) fluence of 2×10^{21} atoms/cm^2 and about 8300 equivalent vacuum ultraviolet Sun hours. AO and UV exposures were taken simultaneously and cell efficiency was retested after AO/UV exposure. Photographs were taken to document regions of interest that might be degraded from AO exposure. Photographs indicated some of the Tedlar was eroded after AO/UV exposure test. Finally, the array was delivered back to the Plasma Interaction Facility (PIF) for extensive testing in LEO and GEO environments.

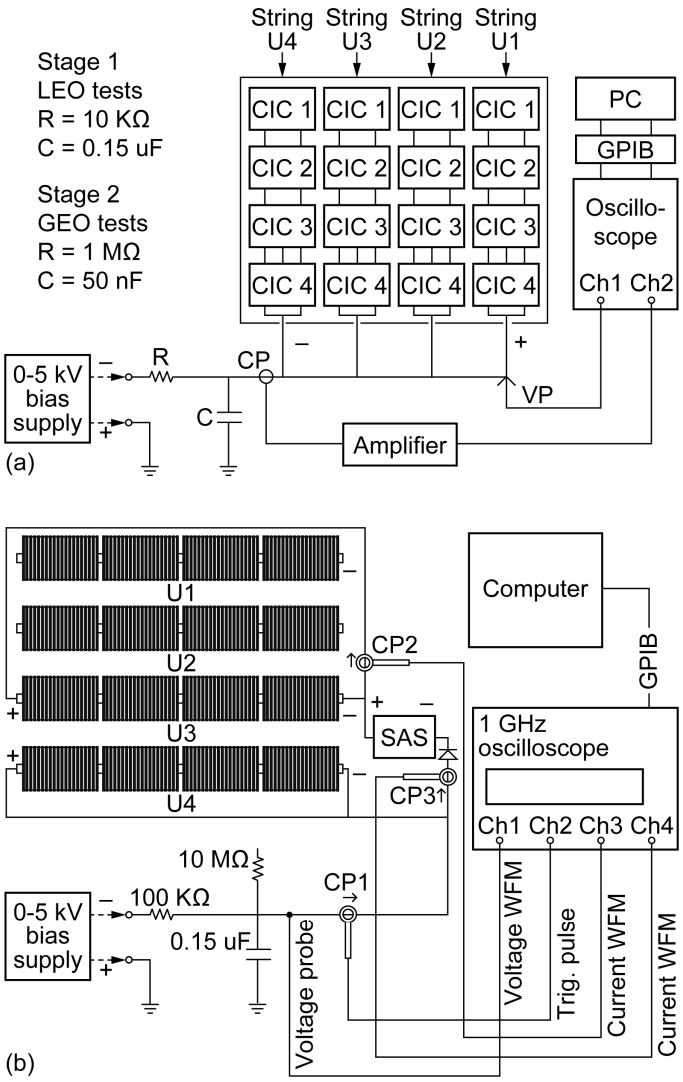

Figure 3.—(a) Primary ESD detection circuitry used for LEO and GEO arc tests. (b) Experimental setup used for sustained arc tests.

Stage 1—LEO Test Procedure Details

Figure 1 shows a single ZTJM array mounted in the chamber. The output leads of each array string were shorted together and connected to a separate high voltage electrical vacuum feedthroughs. Parasitic current for each string was measured separately by sweeping bias voltage within the range of 0 to 120 V. (It is worth noting that the collection current is practically proportional to number density in our range of interest because the Debye radius is much shorter than the sample dimension.) The array bias step voltage was held for 1 s before recording the collection current measurement at each voltage step. Finally, estimates for the parasitic losses were obtained and it was concluded that photovoltaic current losses did not exceeded 0.5 percent. The parasitic current loss estimate applies to the spacecraft 120 V operating voltage. One example of current loss calculations for a single string is shown with the floating potential set at both the 90 and 50 percent operating voltage cases (see Appendix for details).

For the arc threshold tests the bias voltage was initially set to –40 V, and held at this bias level for 60 min. If no arc occurred, the bias voltage was decreased in 10 V decrements and coupon was retested for another 60 min. The procedure was repeated down to the –120 V bias voltage limit. (The arcing threshold limit of –120 V was modified by the test plan committee after the end of the AR-ITO-ZTJM arc

threshold tests. The –120 V limit was replaced by a limit of –240 V as a new margin of safety.) No arc was registered on all four tested samples biased down to 240 V negative. This result negated the necessity of testing against sustained arc inception.

Stage 2—GEO Test Procedure Details

Arcs in GEO are generated by differential charging. Differential charging results from a potential difference between the coverglass and the underlying conductor. When an electron beam irradiates the coverglass surface its potential goes to the steady state magnitude. In order to initiate positive charging of the dielectric the beam energy needs to be higher than the bias voltage. Electrons therefore need to strike the coverglass surface with energy higher than the maximum second electron emission yield (400 to 600 eV). Second crossover energy for most coverglass ranges between 1.2 to 2 kV. So in order to initiate positive charging of the dielectric, the beam energy needs to be about 0.6 to 0.8 kV higher than the array bias voltage. Practically however differential charging depends on a combination of array bias voltage, e-beam energy and secondary electron emission yield (Ref. 13).

For the Stage 2 GEO tests procedure all array strings are shorted together and connected to the negative terminal of a grounded high voltage power supply. Initially, the array bias, V_B is set for –1 kV and the electron gun beam energy, E_B is set to 1.8 keV before proceeding. The beam current densities for both electron guns are initially set to 1 nA/cm^2 and the array sample is irradiated for 30 min. If an arc occurs during this time span, the array fails to meet the arc frequency criteria. If no arcs are detected at the end of the 30 min irradiation test, the beam current flux density is increased to 2 nA/cm^2 and the array is allowed to sit under irradiation for another 30 min. All four samples underwent the GEO tests with current densities of 1, 2, and 5 nA/cm^2, and bias voltages of 1, 2, 3, and 5 kV.

LEO and GEO Test Results

Visual inspections of each array showed no cracks or imperfections to the CICs assemblies, but pointed out a number of other abnormalities: large exposed conductive strips need to be insulated, and the Vectran gore mesh needs to be under greater tension to provide a flat surface to affix cell assemblies. Slight modifications were made to each array sample at the PIF Lab prior to installation in the VF-20 chamber. These modifications consisted of applications of adhesive backed Kapton tape to cover up the nonflight-like bus bars and exposed parts of connecting strips in order to decrease errors in the collection current measurements. Kapton tape was also added along the sides of the Vectran gore mesh not properly affixed to the frame. LEO string current collection was measured by individually biasing each string and sweeping bias voltage between 0 and 120 V in one volt steps using a sensitive sourcemeter to record the current at each voltage step. Current collection was measured for the front and back sides of each of the four UltraFlex arrays. Collection current results are plotted for front side of the AR-ITO-ZTJM CICs sample in Figure 4(a). Front and back side current collection results are plotted for the second AR-ZTJM coated CICs, Figure 4(b). Similar plots for the front and back side of the two AR-ITO-XTJ coated and AR-XTJ coated array CICs are shown in Figures 4(c) and (d). Front side current collection results are plotted separately for all AR-ITO and AR coated array sample assemblies. Current collection curves are plotted for the AR-ITO-ZTJM in Figure 4(e) and for the AR-XTJ array samples in Figure 4(f). The AR-ITO-ZTJM coated array CICs collect 1.7 to 2 times more current (110 V) than CICs coated only with AR layer. The current collection plots (Figs. 4(e) and (f)) illustrate that the ZTJM array CICs tend to collect slightly more current than the arrays XTJ. More quantitative array current collection results are conveniently summarized in Table 2.

LEO arc threshold tests were performed in separate consecutive 1 hr runs with decreasing negative array bias voltages (–10 V steps) down to the maximum level of 240 V negative. Because there were no primary arcs detected during any of the LEO arc threshold tests, no tests were needed to check against the possibility of sustained arcs. Final LEO arcing threshold test results are shown in Table 3.

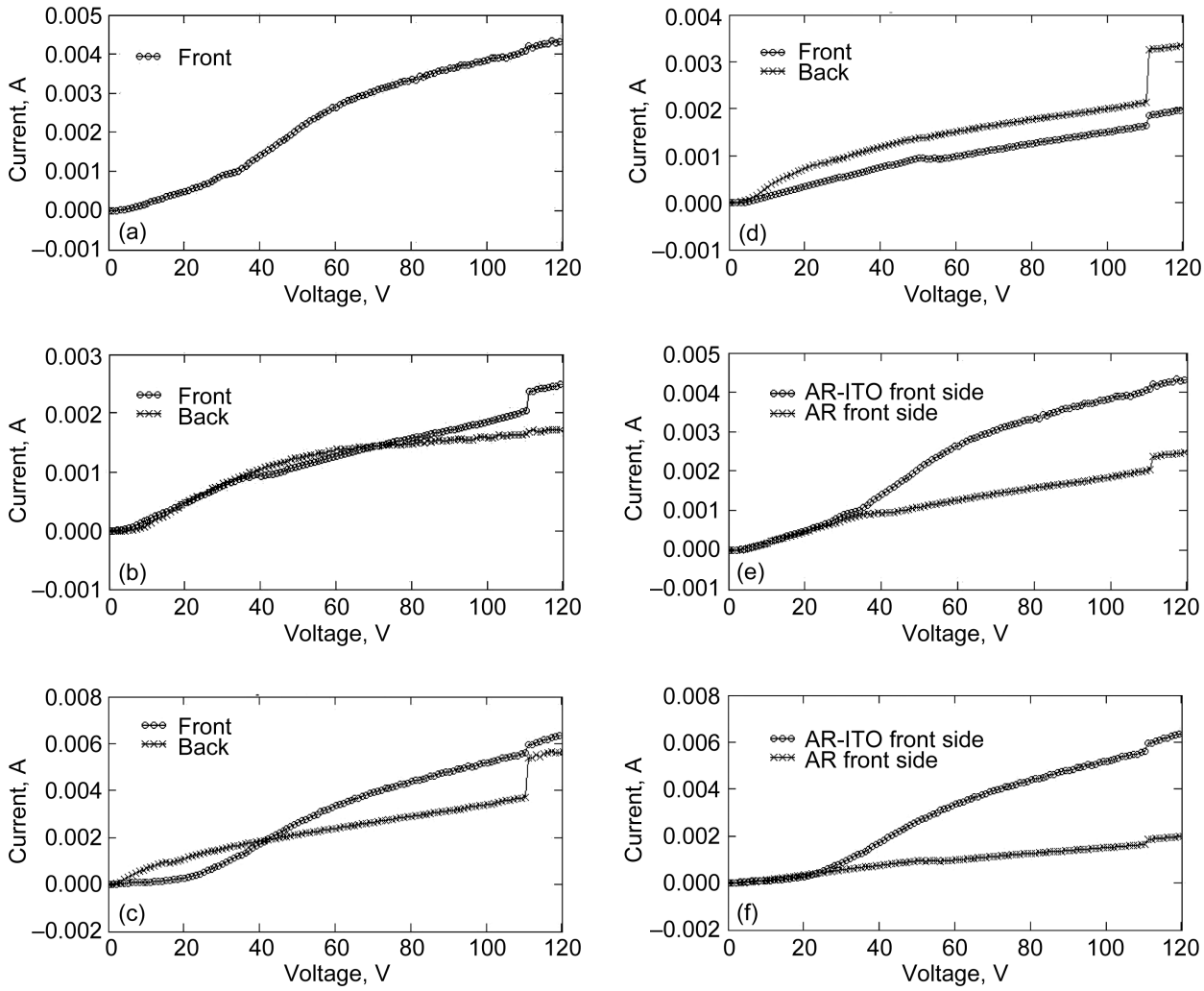

Figure 4.—(a) Collection current for AR-ZTJM CICs front. (b) Current collection for AR-ZTJM-ITO coated array CICs. (c) Current collection for AR-XTJ coated array. (d) Current collection for AR-ITO-XTJ coated array. (e) Front side current collection for ZTJM array CICs. (f) Front side current collection curve for XTJ coated CICs.

TABLE 2.—SUMMARY OF COLLECTED CURRENT RESULTS SCALED TO FLIGHT CONDITIONS FOR AN ORION 28-V POWER SYSTEM

Coupon	Current collected in A at 10 V (25 percent of max string Vop of 35 V)	Equivalent 19-cell string level current collection, A	Successful test?	Comments
AR-ZTJM	0.00030 front	0.00018	Success	Higher collected current than AR-ITO coupon Collected current difference increases to a factor 2x at 50-V bias.
AR-ITO-ZTJM	0.00025 front + 0.00016 back = 0.00041 total	0.00026	Success	
AR-XTJ	0.00020 front + 0.00030 back = 0.00050 total	0.00030	Success	
AR-ITO-XTJ	0.00020 front + 0.00075 back = 0.00095 total	0.00059	Success	Current collected is above 0.00040 A goal but is still an acceptably small value of 0.15 percent of the string operating current.

TABLE 3.—LEO ARC THRESHOLD TEST RESULTS

Coupon	Arc at most negative bias required (–80 V, driven by mated-ISS case)? Yes/No	Arc at most negative bias tested? Yes/No	Successful test?	Comments
AR–ZTJM	No	No (to –120-V)	Success	Good margin demonstrated
AR–ITO–ZTJM	No	No (to –240-V)	Success	Very good margin demonstrated
AR–XTJ	No	No (to –240-V)	Success	Very good margin demonstrated
AR–ITO–XTJ	No	No (to –240-V)	Success	Very good margin demonstrated

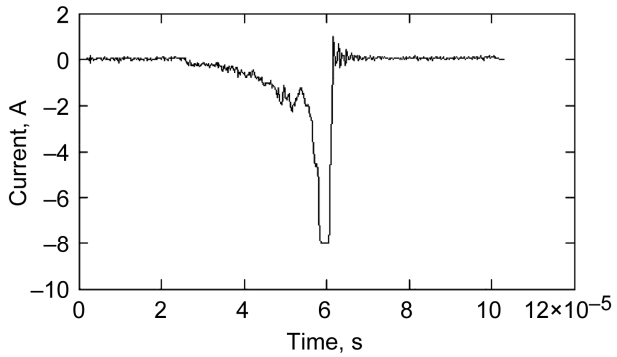

Figure 5.—Example of arc pulse on dielectric Tedlar covering conducting strip. Charging due to e-beam exposure at low beam energy of 1.1 keV and beam current density of 1 nA/cm^2.

GEO Results: AR-ITO-ZTJM Coated Array

All four array strings were shorted together and connected to a High Voltage power supply through the R-C circuit shown in Figure 3(a) (resistor and capacitance values in the R-C circuit were R = 1 MΩ, and C = 50 nF). A problem developed early on in the tests. A number of arcs were registered on the nonflight like areas on the front of the development level array assembly, even at the lowest levels of charging. Discharges were registered in less than 1 min after starting array sample irradiation. Peak current reached 8 A with pulse width of about 10 μs (Fig. 5). An electrostatic probe scan of the cell surfaces showed no signs of differential charging; thus, the ITO layer was effectively bleeding off charges. The sample was re-irradiated by energizing the Electron Gun (EG) using the same array bias potential, beam energy and current density settings, and ten more discharges were generated. Arc sites were clearly located: arcs occurred on the exposed thin Teflon sheet and on the Tedlar dielectric coatings. At this point the decision was made to modify the array by covering all exposed Tedlar strips on the front of the array with Kapton tape (Fig. 6). No modifications were made to the back side of the array. These modifications only allowed testing CICs area on the array sample. Even with the Kapton modifications implemented on the Emcore array arcs still struck on the nonflight like array area (see Fig. 7 for details).

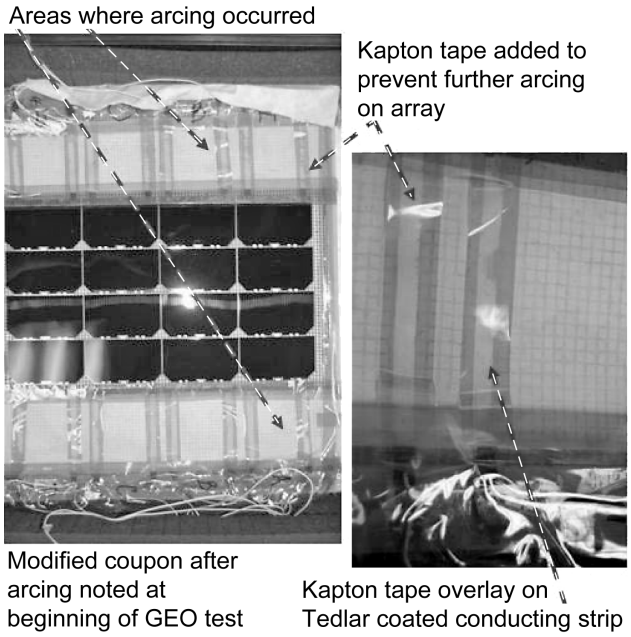

Figure 6.—Modifications made to the ZTJM and XTJ (AR and AR-ITO) UltraFlex array samples.

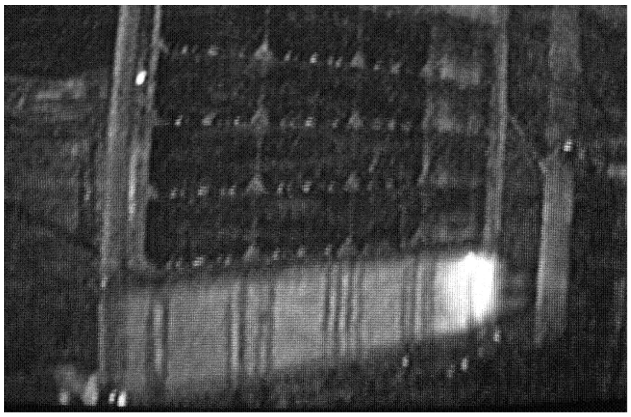

Figure 7.—Snapshot of arc on Tedlar strip triggered with array bias –2.9 kV bias, beam energy 3.5 keV and electron gun current density 7 nA/cm^2.

No surface charging was found at current densities 1, 2, and 5 nA/cm^2 and beam energy up to 3.5 keV. The array was next biased at –2.9 kV negative and irradiated with electron beam energy 3.5 keV and current density of 7 nA/cm^2. Kapton tape strips were charged and an arc discharge occurred on the Kapton covered Tedlar strip (Fig. 7). Sample was dismounted from the VF-20 chamber and brought to calibration laboratory. There was no indication of visual damage or burn marks were found on the sample. The Calibration Laboratory recorded a loss of efficiency in each of the four strings. After the sample was returned a last attempt was made at biasing the array sample at –2.9 kV and irradiating the sample with a beam energy of 3.5 keV and beam current density of 7 nA/cm^2 for a 5 min exposure. Electron gun power supplies were shut down and an electrostatic probe scan was performed directly after e-beam exposure. Horizontal distance between points is 2.2 mm in Figures 8(a) and (b). The electrostatic probe scan clearly demonstrated charging of Kapton tape and a complete absence of charging on any of the CICs array surfaces whatsoever (Fig. 8). The AR-ITO-ZTJM array coupon successively passed all Stage 2 GEO tests. GEO tests were not performed on the back side of the AR-ITO-ZTJM array.

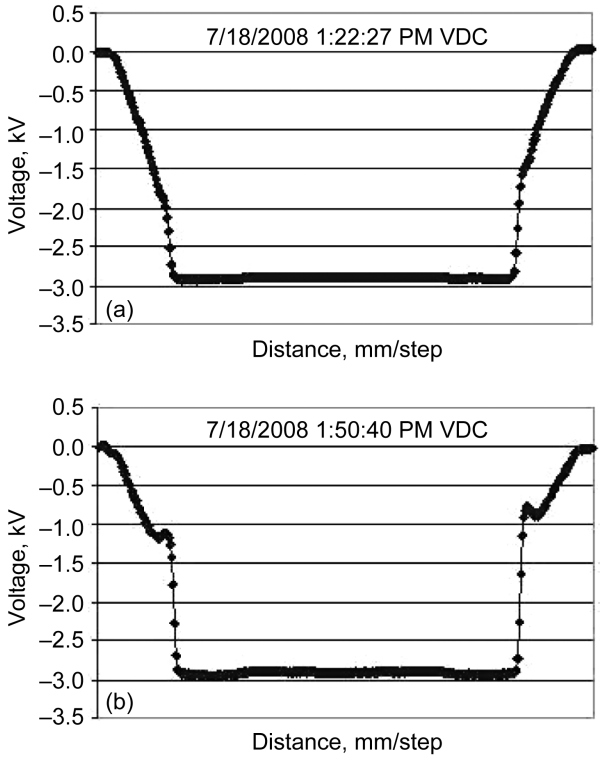

Figure 8.—(a) Electrostatic probe surface scan with array biased at –3 kV but not irradiated. (b) Electrostatic surface potential scan after 5 min irradiation at with V_B = –3 kV, E_B = 3.5 keV and I_B = 7 nA/cm2.

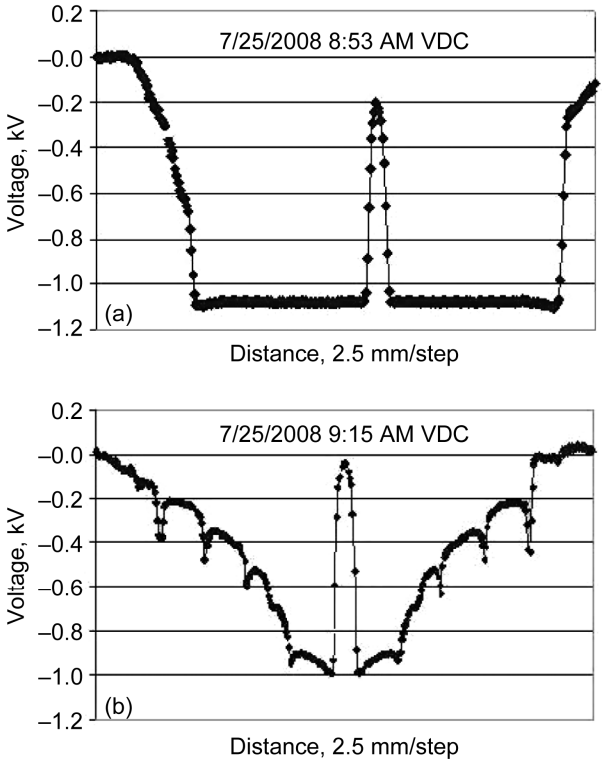

Figure 9.—(a) Surface probe scan of AR-ZTJM coupon indicated a potential of –1.1 (±0.05) kV before irradiation. (b) Differential potential of about 900 V after irradiation.

GEO Results: AR-ZTJM Coated Array

Initially the Emcore AR array was biased at –1.1 kV. Note that the top cell (cell 1) on the array string U4 was cracked, while trying to remove section of Kapton tape which fell on the cell. Figure 9(a) shows an example of a surface probe scan of potentials for the AR-ZTJM array biased at 1.1 kV, but not irradiated. Figure 9(b) shows a surface scan of potentials after irradiation, with the array still biased at –1.1 kV under an e-beam using a beam energy of 1.8 keV and with beam current density of 2 nA/cm^2. No arcs were detected but a scan of surface potentials shows the Emcore AR coated array appears to have acquired differential charging of CIC on the order of 900 V, which clearly indicates that no ITO layer is present on the CIC assemblies. Beam current density was increased to 5 nA/cm^2 and one arc occurred on the cracked cell. String U4 was removed from the circuit. Continued irradiation at the previous beam current density showed no arcing occurred. Array bias level was increased to –2 kV with the beam energy was raised to 2.8 keV and the sample was tested at beam current densities 1, 2, 5, and 10 nA/cm^2 with no arcs detected on the flight like cell surfaces. However, three arcs were triggered on the nonflight like array (first two arcs occurred on the Teflon sheet and the third arc was detected on the Kapton covered Tedlar strip). Resumed testing with the array biased at –3 kV, beam energy 3.5 keV and a beam current density of 2, 3, and 5 nA/cm^2 with no arcs detected on the flight like areas of the AR-ZTJM array. Beam current density was increased to 10 nA/cm^2 and a discharge occurred in the area covered by Kapton tape after 10 min of irradiation (Fig. 10). Note: four lighted CICs above arc site in Figure 10 appear to be due to current flowing through the array string CICs.

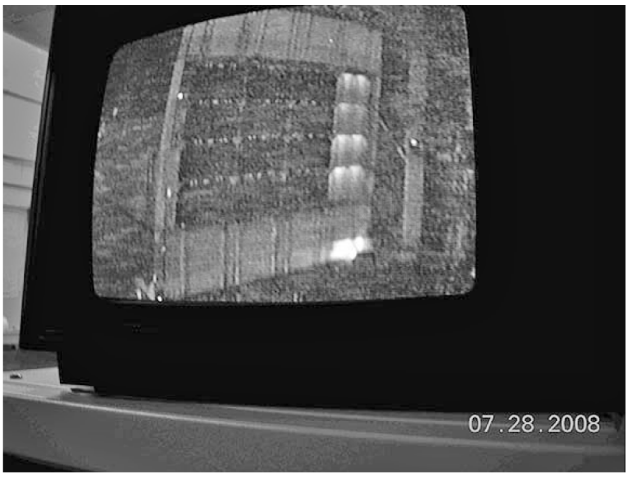

Figure 10.—Discharge on Teflon at –2 kV bias voltage with beam energy at 2.8 keV and with a beam current density of 10 nA/cm2.

The chamber was opened and additional Kapton covers were added to areas of the composite frame and connecting strips. Array sample bias was increased to –3 kV and irradiated with a beam energy of 3.5 keV with a current density of 2 nA/cm^2. The first arc occurred on the string U2 interconnect between CICs 3 and 4. A probe scan of surface potentials indicated differential charging up to 1.5 kV. Beam current density was increased to 3 nA/cm^2 and another arc occurred on the interconnect between CICs 3 and 4 on string U1. Beam current was increased to 5 nA/cm^2 and an arc occurred between cell 3 on string U1 and cell 3 on string U2. A final arc was detected about 15 min later on string U3 between CICs 2 and 3. Therefore, the front side of the AR coated ZTJM array failed to pass Stage 2 GEO tests due to arcing on the flight like areas of the array.

The chamber was opened and the ZTJM array was reinstalled with the electron guns pointed directly at the back side of the array. Back side testing started the –2 kV array bias. No arcs were detected in a 17 min test under irradiation with beam energy of 2.8 keV and beam current density of 5 nA/cm^2. Bias level of the array was increased to –3 kV with beam energy set to 3.5 keV and a beam current density of 1 nA/cm^2. One arc occurred near the top left side of the Kapton cover. Two more arcs were detected on the back side of the array in the area on the conducting strip near the edge of the composite frame. Array bias voltage was increased to –5 kV and the back side of the array was irradiated with e-beam energies of 5.7 keV with a current density of 5 nA/cm^2. Three more arcs were recorded: one arc occurred near the top middle region of the array on the Kapton cover applied over the composite frame and the other two arcs on the Vectran gore mesh near to the string conducting strips. A final attempt was made to see the effects of charging the back side of the array at extreme GEO levels well beyond those expected during flight. For this test the array sample was biased at 9.5 kV and the back side of the array was irradiated with a beam energy of 10 keV and a current density of 10 nA/cm^2. This extreme charging test resulted in multiple number of very intensive arc discharges scattered over face of the back side of the array (Fig. 11).

Figure 11.—Snapshot of AR-ZTJM coated array showing multiple discharges under –9.5 kV bias and irradiated with 10 keV beam energy and 5 nA/cm^2 beam current density.

GEO Results: AR-ITO-XTJ Coated Array

All four strings were biased at –2 kV potential, and TREK probe scan was performed across the surface of the array. Array surface was next irradiated with e-beam energy of 2.5 keV with an e-beam current flux of 2 nA/cm^2. No arcs occurred in the 20 min allotted time interval. Surface potential scan demonstrated that the ITO layer effectively prevented differential charging (Fig. 12). Beam Current density was increased to 5 nA/cm^2 and no arcing occurred at the –2 kV bias level. Bias voltage was then increased to –3 kV and exposed to e-beam and irradiated for 15 min with beam energy at 3.5 keV and an e-beam flux of 5 nA/cm^2. One occurred at dielectric and conductor junction located at the bottom right corner on the bus bar. Continued irradiation of the sample for another 15 min using the same beam parameters showed that no arcs occurred, and an electrostatic probe scan demonstrated the absence of differential charging of array surfaces. Finally, the array bias and beam energy was increased to –5 kV and 5.5 keV, respectively, using a current beam flux 2 nA/cm^2. No arcs were found during 15 min exposure time. Increasing current flux to 5 nA/cm^2 resulted in multiple discharges appeared to originate at the dielectric and conductor junctions located at the top of the array in Figure 13. Continued sample irradiation for an additional 17 min at the same bias –5 kV level, beam energy 5.5 keV and current flux set to 5 nA/cm^2 with no arcs being registered. An extended 1 hr test of the sample with the same parameters resulted in five arcs being registered, all occurring on the nonflight like dielectric and conductor junctions located at the bottom of the array. The front side flight like array segments of the AR-ITO-XTJ array successfully passed the Stage 2 GEO tests. The ITO layer bleeds charge perfectly, but arcing appears to result from adjacent dielectric (Kapton) and conductor (ITO) junctions.

The chamber was opened and the array was mounted with the back side facing the electron guns. When testing resumed the back side of the array was biased at –2 kV and irradiated at beam energy of 2.5 keV and beam current flux of 5 nA/cm^2 in 30-min test. Four arcs were registered on back of the array. The bias level was then increased to –3 kV and irradiated with a 3.5 keV beam having a beam current flux of 5 nA/cm^2 which resulted in four more arc discharges being registered. One example of an arc on the back side of the array is shown in Figure 14. As a result the back side of the Spectrolab AR-ITO-XTJ array failed to pass the Stage 2 GEO tests.

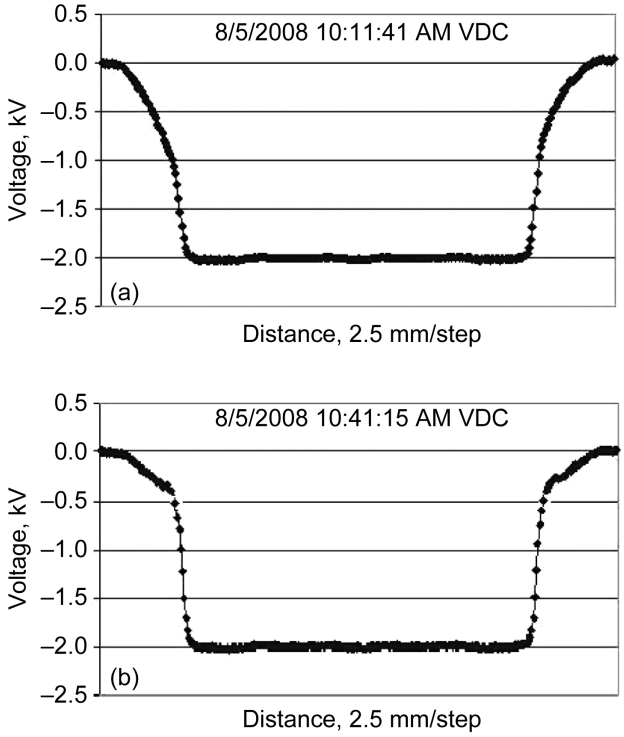

Figure 12.—(a) Surface potential scan with array biased at –2 kV. (b) Surface potential scan after irradiating biased array with e-beam energy of 2.5 keV and beam flux of 2 nA/cm^2.

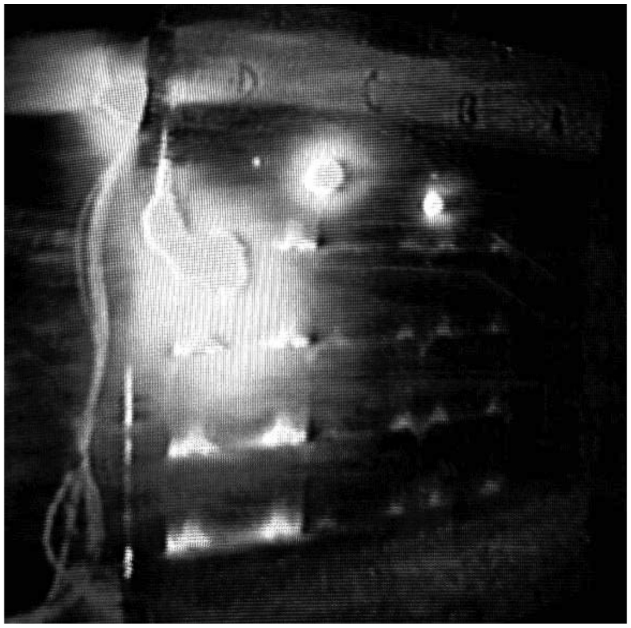

Figure 13.—Multiple discharges at bias potential –5 kV, beam energy 5.5 keV, and beam current flux of 5 nA/cm^2. The discharges are located on the cable leads.

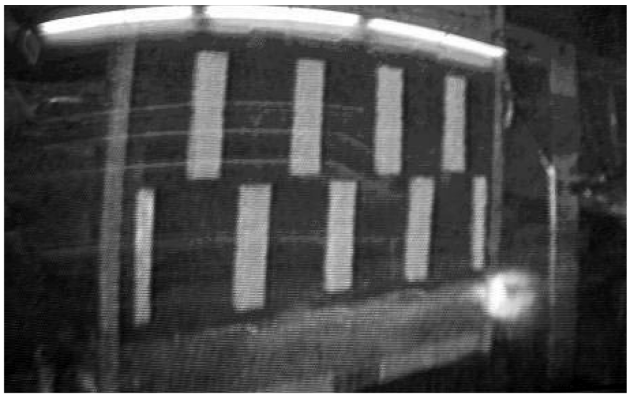

Figure 14.—Arc discharge on the backside of the AR-ITO-XTJ coated array. Arc initiated at –2 kV bias and irradiated at 2.5 keV energy using a 5 nA/cm2 current flux.

AR GEO Results: AR-XTJ Coated Array

Output leads of all the four strings of the AR-XTJ array was connected to the negative terminal of the high voltage power supply through the R-C network (Fig. 3). All four array strings were biased at –2 kV and a surface potential scan was performed before irradiating the array assemblies (Fig. 15(a)). The array was then irradiated with 2.8 keV and 1 nA/cm^2 beam. First arc occurred on the top right corner of array string U1 and a second arc occurred at the same site after 2 min of irradiation. A third arc was recorded at the same position as the first two arcs some 7 min later. Beam current was increased to 3 nA/cm^2. One arc was registered on the bus bar at the top of string U3. After total of 10 min under irradiation, an electrostatic probe scan indicated differential charging of approximately 800 V (Fig. 15(b)).

One arc occurred at the top right corner of the array. The e-beam flux was increased to 5 nA/cm^2 and a second arc was triggered at the same location. The vacuum chamber was opened and both bus bars were covered with Kapton tape. The sample was reinstalled in the chamber and allowed to pump down to the base operating pressure. Testing resumed by biasing the array at –2 kV and irradiated with a beam energy of 2.8 keV and e-beam current flux of 5 nA/cm^2. An arc discharge was initiated between CICs 1 and 2 on string U1 after 7 min under irradiation. The bias voltage, beam energy and current flux was increased to –3 kV, 3.6 keV, and 2 nA/cm^2 and another arc was registered at the same location (top right corner of string U1) after 3 min of e-beam exposure. Increasing the e-beam current flux to 5 nA/cm^2 resulted in four more arcs. Figure 16 shows a plot of current pulse recorded for the fourth arc discharge. As a result the front side of the AR-XTJ coated array failed to pass the Stage 2—GEO tests.

The chamber was opened and the AR-XTJ coated array was pointed with the back side of the array facing the two electron guns. Arc discharges began to be registered at a bias voltage set to –3 kV and when subsequently exposed to e-beam irradiation using beam energy of 3.6 keV and a current density of 2 nA/cm^2. A snapshot taken from the video record of an arc discharge on the back side of the array is shown in Figure 17. Beam current flux was next increased (5 nA/cm^2) at the same beam energy and array bias potential. Another arc discharge was initiated on the back side of the array. As a result the back side of the AR-XTJ array sample also failed to pass Stage 2—GEO tests. A summary of front and back side Stage 2 GEO tests results for all ZTJM and XTJ arrays tested is given in Table 4.

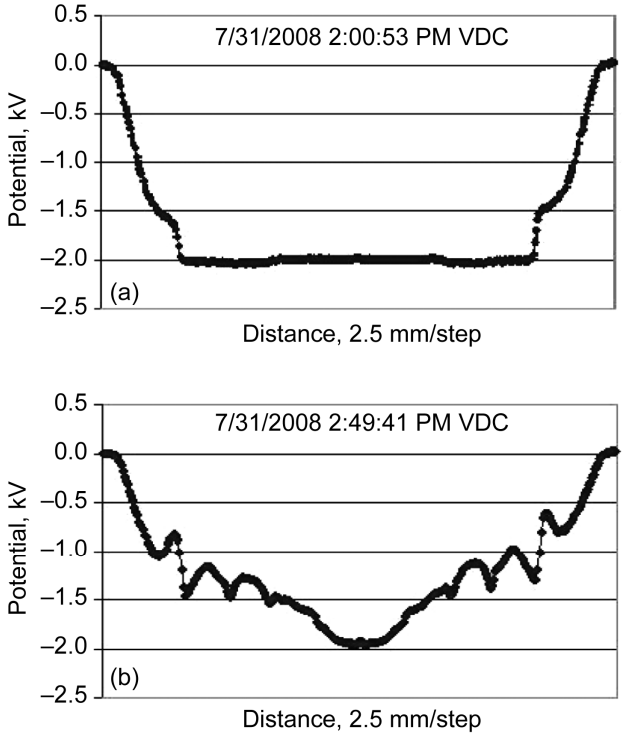

Figure 15.—(a) Surface potential scan with array biased at –2 kV. (b) After 10 min of irradiation with beam energy of 2.8 keV and beam flux 3 nA/cm^2.

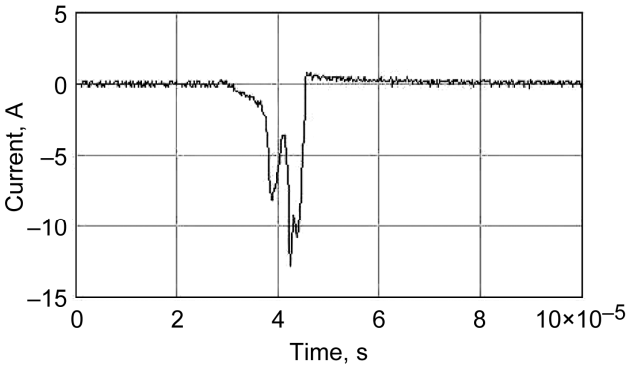

Figure 16.—Current pulse registered at –3 kV bias, beam energy 3.6 keV and current flux of 5 nA/cm^2.

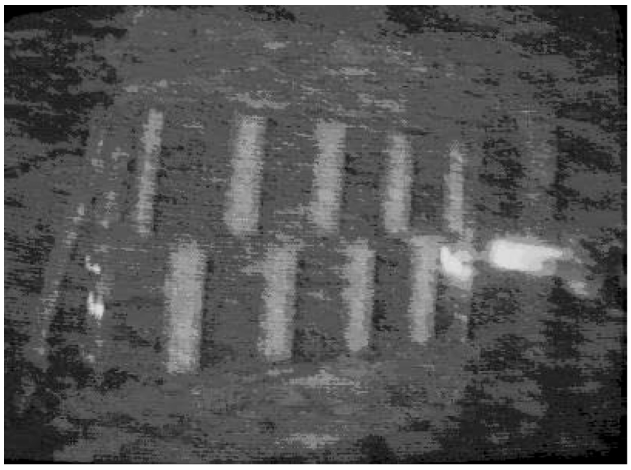

Figure 17.—An arc discharge on backside of AR-XTJ coated array. Discharge recorded using a bias –3 kV under e-beam irradiation energy 3.6 keV and current flux 2 nA/cm2.

TABLE 4.—SUMMARY OF STAGE 2—GEO TESTS FOR FRONT SIDE AND BACK SIDE OF ALL FOUR ZTJM AND XTJ ULTRAFLEX ARRAY SAMPLE ASSEMBLIES

CICs	Arcing at or below most negative bias and e-beam charging parameter tested? Yes/No	Any arcing margin? Yes/No	Successful test?	Comments
ZTJM AR–ITO				
Front to e-beam:	No (up to –3 kV, 3.5 keV, 7 nA/cm^2, 0 V differential charging)	Not tested	Successful[1]	CICs with ITO on the cover show a complete lack of differential charging under e-beam exposure as confirmed by electrostatic probe data. Arcing occurred on nonflight array cabling at –1.1 kV bias, 2 keV energy and 1 nA/cm^2 flux. ~10 A. Arcs caused degraded IV performance of array.
Back to e-beam:	Not tested	Not tested	Not tested	
ZTJM AR				
Front to e-beam:	Yes (at –3 kV, 3.5 keV, 2 nA/cm^2, 1.5 kV differential)	No	Unsuccessful	CICs without ITO on the coverglass are subjected to large differential charging under e-beam exposure. Arcing occurred on nonflight cabling at –1.1 kV bias, 2.8 keV energy and 5 nA/cm^2 flux. 10 A arcs degraded array IV performance.
Back to e-beam:	No (up to –5 kV, 5.7 keV, 5 nA/cm^2)	Yes (arcs at next test point of –9.5 kV, 10 keV, 5 nA/cm^2	Successful	
XTJ AR				
Front to e-beam:	Yes (–2 kV, 2.8 keV, 1 nA/cm^2, 0.8 kV differential)	N/A, not tested	Unsuccessful	Coupon arced at string termination point on round wire cable. CICs arced at –2 kV, 2.8 keV energy and 5 nA/cm^2 flux. Differential bias 1.3 kV.
Back to e-beam:	Yes (–3 kV, 3.6 keV, 2 nA/cm^2)	N/A, not tested	Unsuccessful	
XTJ AR–ITO				
Front to e-beam:	No (up to –5 kV, 5.5 keV, 5 nA/cm^2, 0-V differential)	N/A, not tested	Successful[2]	Coupon arced at string termination pad and at the connection point with round wire cable. Array bias –3 kV under e-beam exposure. 3.5 keV energy and beam 2 nA/cm^2.
Back to e-beam:	Yes (2 kV, 2.5 keV, 5 nA/cm^2)	N/A, not tested	Unsuccessful	

Conclusions

Generally speaking, all ZTJM and XTJ UltraFlex (AR and AR-ITO coated), development level array coupon designs successfully passed the Stage 1 LEO tests results, showing no signs of arcing at ambient test temperature down to –240 V array bias. The AR and AR-ITO coated ZTJM and XTJ CICs and interconnect regions appear to be well designed for operating ESD free in LEO plasma environment. Furthermore, the reported current collection measurements are low (~4 mA) even for the AR-ITO-XTJ coated array sample which collects slightly more current than the ZTJM array; thus parasitic current loss should not be an issue for either of these arrays as part of an Orion 120 V power system. The front side of the ITO coated CIC samples from ZTJM and XTJ arrays also appear to be suitable for use in the GEO charging environments because the ITO coated array CICs did not arc on the front side flight like regions of the array. (Surface potential scans after e-beam irradiation show that the ITO layer effectively bleeds off the charge.) ZTJM and XTJ CIC assemblies layered with ITO are extremely promising in mitigating differential charging effects on the front side of the array, but require some flight design refinements in order to improve the safety of operations in the GEO and Lunar mission environments. For example, minor design changes are needed to eliminate differential charging effects on the Teflon mask and the Tedlar dielectric coatings. String termination pads and wiring need to be redesigned to eliminate arcs the respective regions of the array. Back side of the array CICs needs to have a controlled, minimal amount of silicone insulation in order to prevent arcing in GEO. Arcing occurred at nonflight-like heavy, continuous mesh adhesive regions that allowed for high charging potential compared the same adhesive on the sparse mesh over the solar cell back sides. The coupon back side material GEO charge surface potential scan data showed this behavior. The current test results have provided much valuable information concerning the expected complex charging behavior and survivability of the Orion CEV UltraFlex array design in both the LEO and GEO mission environments. Future tests are planned to explore coupon arcing characteristics over a wider range of operating temperatures and bias voltages. Also, plasma interaction testing with higher fidelity Orion UtraFlex solar array assemblies are planned for the future. In conclusion, a single UltraFlex photovoltaic array can be designed to satisfactorily cope with extended operations in LEO and GEO environments provided design refinements are implemented to improve robustness against arcing.

Appendix—Example Calculation of Parasitic Current Loss for a Single String

Parasitic current loss, I_c for a single string is compared against photovoltaic current loss, I_p and is expressed as a simple ratio I_c/I_{pv}. The string operating voltage V_{op} = 120 V and floating potential, V_f is assumed to be 90 percent of the string operating voltage, V_f = 108 V. The positive voltage peak, V_{pv} = (V_{op}-V_f) or V_p = 12 V potential. A collected current plot versus voltage (from actual data) is given for Spectrolab XTJ-AR array string U1.

The collected string current, I_c is integrated over the entire plot, at a positive peak voltage value, V_{pv} = (V_{op}-V_f) = 12 V. I_c is calculated from Equation (1):

$$I_c = \frac{1}{V_{pv}} \int_{i=0}^{v_{pv}} I(v)\,dv = \frac{1}{12} \sum_{k=1}^{12} I_i(v_i) \tag{1}$$

Therefore, the collected current value yields: $I_c = 7.1 \times 10^{-5}$ A

Assuming the peak current, I_{pv} from a single string is I_{pv} = 0.5 A then I_p gives the gives the required ratio for calculating the magnitude of the parasitic current loss of string U1 in Equation (2):

$$I_p = \frac{I_c}{I_{pv}} = \frac{7.1 \times 10^{-5}}{0.5} = 1.1 \cdot 10^{-3} = 0.00014\,\% \tag{2}$$

If the floating potential, V_f is now assumed to be 50 percent of the operating potential, V_{op} = 120 V then V_f = (0.5)(120) = 60 V and the positive peak voltage, V_{pv} = (120-60) = 60 V. The collected current, I_c computed from the curve is then specified in Equation (3):

$$I_c = \frac{1}{V_{pv}} \int_{i=0}^{v_{pv}} I(v)\,dv = \frac{1}{60} \sum_{k=1}^{60} I_i(v_i) \tag{3}$$

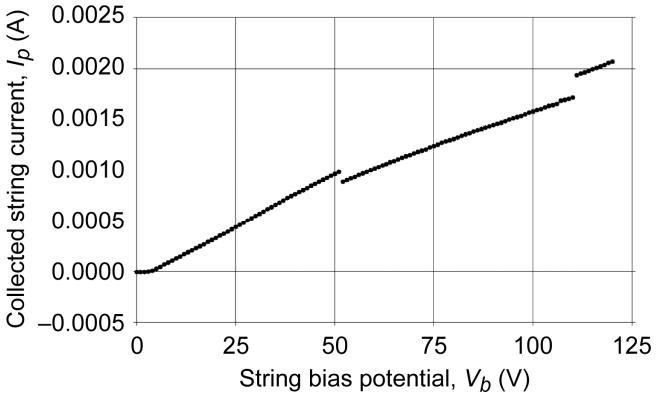

Figure 18.—Collected current plot for ZTJM AR-ITO string U1.

The value of the collected current I_c now becomes

$$I_c = 5.5 \cdot 10^{-4} A$$

The parasitic current loss, I_p from string U1 can then be similarly computed from the ratio in Equation (4):

$$I_p = \frac{I_c}{I_{pv}} = \frac{5.5 \times 10^{-4}}{0.5} = 1.1 \cdot 10^{-3} = 0.11\% \tag{4}$$

References

1. White, S.; Douglas, M.; Spence, B.; Jones, P.A.; Piszczor, M.F., "Development of an ultraflex-based thin film solar array for space applications," 2003, Proceedings of 3rd World Conference on Photovoltaic Energy Conversion, vol. 2, May 2003, pp. 793–796 vol. 1.
2. Spence, B., White, S., Wilder, N., Gregory, T., Douglas, M., Takeda, R., Mardesich, N., Peterson, Hillard, Sharps, P., and Fatemi, N., "Next Generation UltraFlex Solar Array for NASA's New Millennium Program Space Technology 8 (ST8)," 31st IEEE Photovoltaic Specialists Conference, Jan. 2005, 2005, pp. 826–829.
3. Sharps, P., Aiken, D., Stan, M., Cornfeld, A., Newman, F., Endicter, S., Hills, J., Girard, G., Doman, J., Turner, M., Sandoval, A., and Fatemi, N., "Space Solar Cell Research and Development Projects at Emcore Photovoltaics," NASA/CP—2007-214494, pp. 145–152.
4. Fetzer, C.M., King, R.R., Law, D.C., Edmondson, T., Isshiki, M., Haddad, J.C., Boisvert, J.C., Zhang, X., Joslin, D.E., and Karam, N.H., "Multijunction Solar Cell Development and Production at Spectrolab," NASA/CP—2007-214494, pp. 153–159.
5. Spence, B.; White, S.; Jones, A.; Wachholz, J.; Wilder, N.; Cronin, P.; Gregory, T.; Barker, P.; Allmandinger, T.; Mardesich, N.; Piszczor, M.; Sharps, P.; Fatemi, N., "UltraFlex-175 Solar Array Technology Maturation Achievements for NASA's New Millennium Program (NMP) Space Technology 8 (ST8)," IEEE 4th World Photovoltaic Energy Conversion Conference, vol. 2, WCPEC—2006-279879, May 2006, pp. 1946–1950.
6. Hillard, G., Vayner, B., Galofaro, J., Snyder, D., Dever, J.A., and Miller, S.K. "Preliminary Assessment of Environmental Interactions for the Orion Solar Arrays," NASA/TM—2009-215823, June 15, 2007.
7. Ferguson, D., Hillard, G., Snyder, D., and Grier, N., "The Inception of Snapover on Arrays: a Visualization Technique," AIAA Paper 98–1045, Jan., 1998, pp. 1–8.
8. Galofaro, J., Vayner V., Degroot W., Ferguson, D., Thomson, C.D., Dennison, J.R., and Davies, R.E. "Inception of Snapover and Gas Induced Glow Discharges," NASA/TM—2000-209645, Jan., 2000, pp. 1–5.
9. Caven, P., Coffey, V., Schneider, T., Vaughn, J., Wright, K., and Minow, J. "Survey of International Space Station Charging Events," AIAA Paper 2009-0119, Jan. 2009, pp. 1–6.
10. Carruth, M.R. et al., "ISS and Space Environment Interactions Without Operating Plasma Contactor," AIAA–2001–0401, Jan. 2001, pp. 1–7.
11. Schneider, T. et al., 2002, "Minimum Arc Threshold Voltage Experiments on Extravehicular Mobility Unit Samples," AIAA–2002–1040, Jan. 2002, pp. 1–4.
12. Purvis, C.K., Garett, H.B., and Stevens, J.N., "Design Guidelines for Assessing and Controlling Spacecraft Charging Effects," NASA/TM 2361, 1984, pp. 1–46.
13. Vayner, B.V., Ferguson, D.C., and Galofaro, J.T., "Comparative Analysis of Arcing in LEO and GEO Simulated Environments," AIAA–0093–2007, Reno, NV, Jan 2007, pp. 1–18.

REPORT DOCUMENTATION PAGE			Form Approved OMB No. 0704-0188

1. REPORT DATE *(DD-MM-YYYY)*	2. REPORT TYPE	3. DATES COVERED *(From - To)*
01-05-2010	Technical Memorandum	

4. TITLE AND SUBTITLE
Experimental Charging Behavior of Orion UltraFlex Array Designs

5a. CONTRACT NUMBER

5b. GRANT NUMBER

5c. PROGRAM ELEMENT NUMBER

6. AUTHOR(S)
Galofaro, Joel, T.; Vayner, Boris, V.; Hillard, Grover, B.

5d. PROJECT NUMBER

5e. TASK NUMBER

5f. WORK UNIT NUMBER
WBS 644423.06.32.03.05.03

7. PERFORMING ORGANIZATION NAME(S) AND ADDRESS(ES)
National Aeronautics and Space Administration
John H. Glenn Research Center at Lewis Field
Cleveland, Ohio 44135-3191

8. PERFORMING ORGANIZATION REPORT NUMBER
E-17068-2

9. SPONSORING/MONITORING AGENCY NAME(S) AND ADDRESS(ES)
National Aeronautics and Space Administration
Washington, DC 20546-0001

10. SPONSORING/MONITOR'S ACRONYM(S)
NASA

11. SPONSORING/MONITORING REPORT NUMBER
NASA/TM-2010-216751

12. DISTRIBUTION/AVAILABILITY STATEMENT
Unclassified-Unlimited
Subject Category: 18
Available electronically at http://gltrs.grc.nasa.gov
This publication is available from the NASA Center for AeroSpace Information, 443-757-5802

13. SUPPLEMENTARY NOTES
Submitted to Journal of Spacecraft and Rockets.

14. ABSTRACT
The present ground based investigations give the first definitive look describing the charging behavior of Orion UltraFlex arrays in both the Low Earth Orbital (LEO) and geosynchronous (GEO) environments. Note the LEO charging environment also applies to the International Space Station (ISS). The GEO charging environment includes the bounding case for all lunar mission environments. The UltraFlex photovoltaic array technology is targeted to become the sole power system for life support and on-orbit power for the manned Orion Crew Exploration Vehicle (CEV). The purpose of the experimental tests is to gain an understanding of the complex charging behavior to answer some of the basic performance and survivability issues to ascertain if a single UltraFlex array design will be able to cope with the projected worst case LEO and GEO charging environments. Stage 1 LEO plasma testing revealed that all four arrays successfully passed arc threshold bias tests down to -240 V. Stage 2 GEO electron gun charging tests revealed that only the front side area of indium tin oxide coated array designs successfully passed the arc frequency tests.

15. SUBJECT TERMS
Orion; Photovoltaic (PV) array

16. SECURITY CLASSIFICATION OF:			17. LIMITATION OF ABSTRACT	18. NUMBER OF PAGES	19a. NAME OF RESPONSIBLE PERSON
a. REPORT	b. ABSTRACT	c. THIS PAGE			STI Help Desk (email:help@sti.nasa.gov)
U	U	U	UU	27	19b. TELEPHONE NUMBER *(include area code)* 443-757-5802